Journal of Al-Azhar University Engineering Sector

Vol. 20, No. 77, October 2025, 1143-1154

OCEANIC TURBULENCE EFFECT ON UNDERWATER VISIBLE LIGHT COMMUNICATION

Mohammed A. Salem*[,1], Radwa A. Roshdy[1]

Electrical Engineering Department, Higher Technological Institute, 10th of Ramadan city, Egypt.

* Correspondence: mohammed.adel@hti.edu.eg

Citation:

Salem M.A., Roshdy R.A., " Oceanic Turbulence Effect on Underwater Visible Light Communication", Journal of Al-Azhar University Engineering Sector, vol. 20, No. 77, pp. 1143-1154, 2025.

Received: 19 March 2025

Revised: 28 May 2025

Accepted: 19 June 2025

Doi: 10.21608/auej.2025.369737.1799

ABSTRACT

Underwater Visible Light Communication (UVLC) has the potential to replace acoustic/RF systems with high-speed, low-latency oceanic exploration, research, and environmental monitoring links. Turbulence, generated by temperature/salinity gradients and water currents, causes performance degradation through fading and path loss. In this paper, the effect of turbulence is evaluated using a Nakagami-m channel model with consideration of Bit Error Rate (BER) for On-off keying (OOK) and Binary Phase Shift Keying (BPSK) modulations under weak (k=10), moderate (k=3), and strong turbulence (k=0.8). Simulations probe single- and multi-LED configurations in pure, coastal, and turbid waters. Results indicate that multi-LED arrays offer near-error-free links (BER $<10^{-4}$ at 40 dB Signal-to-Noise Ratio(SNR)) in weak turbulence, much better than single-LED configurations by orders of magnitude. Coastal water has the poorest BER due to scattering, with pure seawater having the best performance. Turbulence strength k=0.8 demands higher SNR, indicating the effect of spatial diversity in combating fading. Multi-LED architectures enhance UVLC resilience by dispersing signal routes, reducing turbulence-induced fluctuations. In addition, BPSK demonstrates greater resilience than OOK under high-turbulence regimes. These findings provide critical design insight into building resilient underwater networks, emphasizing spatial diversity and modulation selection to counteract channel degradations. The study finds the feasibility of UVLC in turbulent channels, supporting green solutions to underwater communication issues.

KEYWORDS: Underwater visible light communication, Ocean turbulence, Nakagami distribution, PSK, OOK

تأثير الاضطراب المحيطي على الاتصالات البصرية تحت الماء

محمد عادل راشد سالم*،١، رضوى عادل السيد رشدي١

١ قسم الهندسة الكهربية، المعهد التكنولوجي العالي، مدينة العاشر من رمضان، مصر

البريد الاليكتروني للباحث الرئيسي: mohammed.adel@hti.edu.eg*

الملخص

يعد الاتصال الضوئي المرئي تحت الماء بديلا واعدا للأنظمة الصوتية واللاسلكية حيث يوفر اتصالا عالي السرعة ومنخفض زمن الاستجابة ومع ذلك تؤدي الاضطرابات الناجمة عن تغيرات درجة الحرارة والملوحة وتدفق المياه الى تدهور الاداء من خلال التلاشي وفقدان الاشارة تبحث هذه الدراسة في تأثيرات هذه الاضطرابات باستخدام نموذج ناكاجامي حيث تقارن معدلات خطأ البت لأنظمة التضمين ثنائي النبض وثنائي الطور تحت اضطرابات ضعيفة متوسطة وقوية تحاكي الدراسة تكوينات تعتمد على مصابيح ضوئية مفردة ومتعددة في بيئات مائية مختلفة نقية ساحلية وعكرة تظهر النتائج ان الأنظمة متعددة المصابيح تحقق اتصالا شبه خال من الاخطاء عند نسبة اشارة الى ضوضاء مرتفعة متفوقة بفارق كبير على الأنظمة أحادية المصباح تسجل أسوأ معدلات الخطأ في المياه الساحلية بسبب التبعثر بينما تقدم المياه النقية افضل أداء تؤكد الدراسة ان الهياكل متعددة المصابيح تعزز موثوقية الاتصال في البيئات المضطربة مما يوفر توجيهات أساسية لتصميم شبكات اتصال تحت الماء اكثر استقرارا في مجالات الاستكشاف البحري البحث العلمي ورصد البيئة المائية.

الكلمات المفتاحية : الاتصالات البصرية تحت الماء، الاضطراب المحيطي، توزيع ناكاغامي، تعديل PSK، تعديل OOK

1. INTRODUCTION

Applications ranging from marine research to underwater exploration, military operations to environmental monitoring depend on underwater communication. Underwater conditions provide challenges for conventional means of communication including acoustic and radio frequency (RF) communications [1-3]. While RF signals suffer great attenuation in water, especially at higher frequencies, acoustic waves suffer from weak data rates and acute delay [4]. Underwater Visible Light Communication (UVLC) has shown promise as a means of overcoming these difficulties. UVLC uses visible light (wavelengths between 400–700 nm) underwater data transmission. UVLC allows rapid, low-latency data transfer over short to moderate distances as light travels faster than sound and suffers less attenuation in clear water than RF waves [5]. A data throughput of 3.24 Gb/s was attained by using new two-color laser diodes, therefore underlining the possibilities of laser-based UVLC systems for high-speed underwater transmission [6]. UVLC has problems including absorption and scattering by water, alignment sensitivity, interference from ambient light and turbulence resulting from temperature gradients, salinity changes, and water flow dynamics notwithstanding its benefits. Absorption and scattering, even though described by exponential attenuation functions, in UVLC systems [5] are still reliability-limited on their operational deployment. There have been studies on modulation and signal processing techniques to reduce such effect and enhance the system robustness to such channel impairments [7,8].

1.1. Related Works

Most of the studies have addressed different topics of UVLC like channel modeling, modulation, and the influence of the environment on signal transmission. The impact of sea waves on vertical UVLC links is discussed, therefore giving insight into environmental influences affecting communication performance [9]. A UVLC system employing Phase-Shift Keying (PSK) modulation is suggested, and its applicability underwater is emphasized, facilitating applications in drones [10]. Most notably for the design of effective underwater communication networks, this study offers a thorough examination of route loss in UVLC systems [11]. Examining data transmission and energy harvesting, the performance of several modulation in climatology UVLC under absorption and scattering in underwater communication was surveyed, while the hybrid and adaptive modulation schemes were introduced to improve the BER performance for the optical systems under both absorption and turbulence conditions, highlighting their practical performance for realistic underwater applications [5,7,8]. Simultaneous Lightwave Information and Power Transfer (SLIPT) for UVLC devices is studied [12]. A gain feedback control technique with a dynamic threshold is proposed to improve communication dependability, hence addressing mobility in UVLC systems [13]. Integrating route loss and time variety, the average bit error rate (ABER) performance of Non-Line of Sight (NLOS) ultraviolet connections over strong turbulent channels is assessed. The results imply that temporal diversity methods can efficiently minimize the negative consequences of turbulence on UVLC systems [14]. Vertical UVLC connections under high maritime turbulence were examined using probability density functions to evaluate performance deterioration [15]. Emphasizing difficulties in preserving stable connections, research on the combined impacts of underwater turbulence and wavy water surfaces on water-to-air visible light communication linkages is presented. Using orbital angular momentum (OAM) light and polarization coding to lower bit error rates and lengthen communication lengths, a channel polarization system for ocean turbulence channels was presented [16,17].

1.2. Motivation and Contributions

Underwater VLC is significantly affected by oceanic turbulence, which introduces signal degradation caused by scattering, absorption, turbulence-induced fading, and geometric path loss. This motivated us to Understand this effect is to improv the reliability and efficiency of underwater VLC systems. The main contributions of this paper are:

1. using statistical models to offer an investigation of how ocean turbulence affects VLC signal propagation. Nakagami distribution for On-off keying (OOK) and Binary Phase Shift Keying (BPSK) modulation define the fading effects.
2. analyzing the Bit Error Rate (BER) under various turbulence situations helps one to evaluate the effect of turbulence on system performance and so gain understanding of system dependability.
3. comparing the performance variations between a single LED and several LED setups underlining their efficiency in reducing signal degradation caused by turbulence.
4. providing insightful analysis of building strong underwater VLC systems helps to create more dependable underwater communication networks by means of higher efficiency.

The paper arranged as follows. In section 2, underwater VLC system model under k and Nakagami distributions is presented. In section 3, performance evaluation is shown through simulation results. The conclusion is introduced in section 4

2. SYSTEM MODEL

Fig. 1 shows the block diagram of the UVLC system. The LED array comprises one or more LEDs. Exploiting the spatial diversity that the LEDs can offer (either via a single LED or multiple LEDs) our system transmits a digital bitstream OOK or BPSK modulated. The optical signal is transmitted through the underwater link, where it suffers from an attenuation described by the Beer-Lambert law, as well as from turbulence fading described by the Nakagami-k distribution. The optical signal is detected with a photodetector, and then converted into an electrical signal, which is demodulated by the demodulator and BER measured. This framework simulates the underwater communication environment and system elements in different turbulent environments.

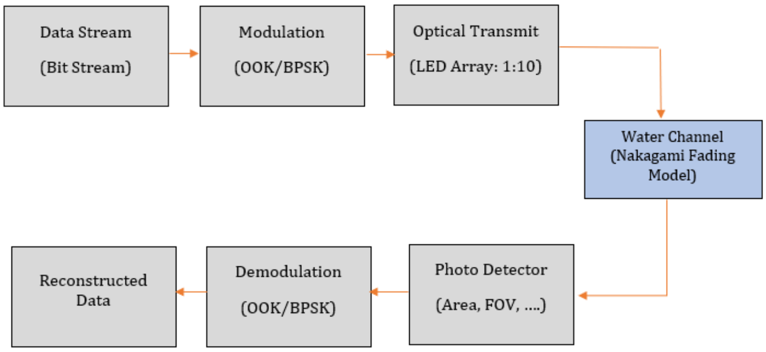

Fig. 1: UVLC system block diagram.

This paper employed a model based on Beer-Lambert equation [18], which incorporates factors including the distance that exists between the two devices, the area of the photodiode (PD), the half-angle, the optical gain, the concentrator gain, and the extinction parameters. The path attenuation in an underwater optical communication channel is influenced by attenuation loss and geometric loss. Attenuation loss, dependent on water type, is modeled using the recognized Beer-Lambert equation.

$$PL_{attenuation} = e^{-c(\lambda)D} \tag{1}$$

where D represents the distance between the two devices, whereas c(λ) denotes the extinction coefficient, which is contingent upon the absorption coefficient, a(λ), and the scattering coefficient, b(λ). The extinction coefficient is articulated as follows [19].

$$c(\lambda) = a(\lambda) + b(\lambda) \tag{2}$$

The geometric loss in the system arises from the transferred beam between the emitter and the PD receiver. This type of loss is based on the attributes of the system and can be represented mathematically as follows [20], [21].

$$PL_{Geometric} = \frac{A_{PD}(m+1)\cos(\phi)^m g(\theta)\, T_s(\theta)\cos(\theta)}{2\pi D^2} \tag{3}$$

In the aforementioned equation, APD represents the area of photodetector, m represents Lambertian order of emission, ϕ is emission angle, θ represents the angle of incidence, g(θ) is optical gain, Ts(θ) is the gain of filter, and D is the range of transmitter and receiver. With the addition of route loss through attenuation and through geometric loss, we can derive the total route loss expressed by the formula below [22].

$$H_{UW} = \frac{A_{PD}(m+1)\cos(\phi)^m g(\theta)\, T_s(\theta)\cos(\theta)}{2\pi D^2} \cdot e^{-c(\lambda)D} \tag{4}$$

This research uses the Nakagami fading framework for turbulence analysis. This model takes underwater turbulence's variances in received optical power into account.

$$f(x;k,\Omega) = \frac{2k^k}{\Gamma(k)\Omega^k} x^{2k-1} \exp\left(-\frac{k}{\Omega}x^2\right) \; for\ x \geq 0 \tag{5}$$

where k represents the form parameter, hence controlling the degree of fading; a higher value of k indicates less fading severity. The spread parameter, Ω, indicates the average power of the observed signal in a signatory sense. Γ(k) expresses the Gamma function. x is the fading coefficient that denotes optical turbulence-induced signal fluctuations.

The Nakagami distribution is used in the present work since it is able to provide flexible models for different turbulence conditions by knowing the shape parameter k; the larger the k (e.g., k = 10), the weaker the turbulence property, and the smaller the k (e.g., 0.8), the stronger the turbulence property of the channel with severe signal fluctuations. The latter approximations are similar to the physical ocean conditions (like temperature, salinity, and flow dynamics) in terms of the known/unknown state, which result to amplitude changes received in the optical signal. The Nakagami model reflects these characteristics and is therefore a useful model to employ to investigate the turbulence effect on an UWA optical channel.

Under communication channels when a dominating Line of Sight (LOS) link is present, the obtained power can be expressed as [23]:

$$P_R = H_{UW} \cdot P_T \tag{6}$$

In the above given sentence, PT stands for the transmitted power and PR for the received power. Three types of noise were investigated in order to determine the Signal-to-Noise Ratio (SNR) of the system: thermal noise, amplifier noise, and shot noise [24]. Shot noise resulting from photon stochastic arrival at the PD was represented with the equation,

$$Noise_{sh} = 2qRP_RB_e \tag{7}$$

where R shows the photodiode's responsivity, and q stands for the electron charge. Referring to the noise the amplifier produced as amplifier noise, the following equation helped to depict it:

$$Noise_{A_m} = I_a^2 B_a \tag{8}$$

where I_a and B_a represent the current, and the bandwidth of the amplifier, respectively. The noise, resulting from the thermal agitating of electrons, was represented by:

$$Noise_{Th} = \frac{4K_bTB_e}{R_s} \tag{9}$$

where K_b indicates Boltzmann's constant, T represents the temperature (290 K) [24], and R_s is the resistance represented by thermal noise originating from the thermal agitation of electrons within the system. Addition of the separate noise components helped one to ascertain the total noise level.

$$Noise_{Total} = Noise_{sh} + Noise_{A_m} + Noise_{Th} \tag{١٠}$$

The SNR was finally computed by:

$$SNR = \frac{(RP_R)^2}{Noise_{Total}} \tag{١١}$$

The efficiency of the UVLC system is sensitive to the intensity of turbulence displaying Nakagami shape parameter k. Operations of the system under weak turbulence (k=10) reveal that a low BER results whether single or multiple LEDs are employed. That is, when the turbulence is under moderate (k = 3) and strong (k = 0.8), the occurrence of the fading is enhanced and so when a number of independent LEDs is employed, a better reliability can be achieved by spatial diversity.

Moreover, BPSK modulated signal, while being less power efficient if compared to OOK, is more resilient to deep fading. The properties of the photo detector, i.e., its size and; field of view, also affect signal reception. The robustness of the system is built on a proper choice of the modulation, the hardware settings and the channel model in such a way that the communication is reliable.

3. SIMULATION RESULTS

This section is intended to show the BER of the UVLC system's performance for both single and multi-LED configurations in different turbulence conditions. The simulations were all carried out through MATLAB R2023a which is a code. The UVLC-system communicates modulated light through an LED-array - which here also can be performed by a single LED or several LEDs to obtain a spatial diversity. Different modulation schemes, such as OOK and BPSK are proposed for the flexibility to react with various degrees of robustness, to the presence of turbulence. The Nakagami-k distribution is used to model turbulence, and the index is the shape parameter of Nakagami probability distribution, of which k=10 is weak, k=3 is average and k=0.8 takes a high level of turbulence. As K values decrease signal amplitude fluctuations become greater. So, by using several LEDs, fading depth is quite reduced through the diversity order. At the receiver end, the optical signal is received by a photodetector and is demodulated to decode original data. The system performance, in terms of the BER, is dependent on the intensity of the turbulence, modulation conditions and the arrangement of LEDs. The full customizability and reproducibility of the process were achieved by setting the parameters through the structure of the code, without GUI use.

Table 1: The simulation parameters

Parameter	Value
Modulation Types	BPSK, OOK
Channel model	Nakagami
Weak Turbulence	K=10
Moderate Turbulence	K=3
Strong turbulence	K=0.8
Number of transmitted bits	106
Refractive Index of the Lens	1.5
Field of View of the Photodiode	70°
Semi-angle of LED at half-power	70°
Area of the Photodiode	0.05
Irradiance angle	40°
Receiver angle	60°
Power of LED	1 Watt
Distance	10 m
Number of LEDs	Single LED, Multiple LEDs=10

Building on **Table 1**, the specific parameter values for the representation of each simulation scenario can be found. These values have been taken from real-life situations and are considered to be valid and real. Furthermore, the qualities of UVLC systems that have been well-documented in the literature have been adopted as well as the rest of the system parameters [23,24].

The parameters of the simulation are based on the values supported by data in the literature. For example, the extinctive coefficient in water types is estimated based on measured values, such as 0.151 m^{-1} in pure seawater (a = 0.114 m^{-1}, b = 0.037 m^{-1}), 0.398 m^{-1} in coastal waters that shows higher scattering and absorption [25]. Furthermore, the experimental results in the Southern Indian Ocean show BER of about10^{-4} when the strong turbulence is experienced with SNR lying from 45 to 80 dB [26]. These observations are consistent with our simulation results and support the credibility of the turbulence and attenuation models employed.

To verify our simulation model, we compared our simulations with those in [15], where they studied the performance of UVLC in moderate turbulence with the help of gamma-gamma distribution. Matching key parameters, we took care of a meaningful comparison. Such benchmarking validates the correctness of the Nakagami fading model and puts in perspective the BER results presented in the next figures.

Figs. 2 and 3 show the BER performance versus SNR for BPSK and OOK at weak turbulence (K=10), moderate turbulence (K=3) and strong turbulence (K=0.8), respectively. **Figs. 4 and 5** depict BER versus SNR of BPSK and OOK for different types of water, namely, pure sea, ocean, and coastal water, respectively**. Figs. 1 to 4** show the BER at single LED and Multiple LEDs.

The BER vs. SNR curve shows the influence of Nakagami-k fading and the number of LEDs on the performance of an UVLC system. For higher Nakagami-k values (k = 10, weak turbulence), the BER is significantly lower, indicating more stable channel conditions, whereas higher turbulence (k = 0.8) generates higher BER for all SNR levels due to the heavy fading. Also, the use of multiple LEDs improves performance by means of minimum BER reduction by using spatial diversity for the mitigation of turbulence-induced ripples. Systems of k = 10 and multiple LEDs achieve very close-to-zero BER at high SNR values (>40 dB), yielding particularly good communication but conditions with high turbulence are still errored, with a more need for high levels of power or advanced signal-processing algorithms.

The BER vs. SNR curve shows the influence of Nakagami-k fading and the number of LEDs on the performance of an UVLC system. For higher Nakagami-k values (k = 10, weak turbulence), the BER is significantly lower, indicating more stable channel conditions, whereas higher turbulence (k = 0.8) generates higher BER for all SNR levels due to the heavy fading. Also, the use of multiple LEDs improves performance by means of minimum BER reduction by using spatial diversity for the mitigation of turbulence-induced ripples. Systems of k = 10 and multiple LEDs achieve very close-to-zero BER at high SNR values (>40 dB), yielding particularly good communication but conditions with high turbulence are still errored, with a more need for high levels of power or advanced signal-processing algorithms.

Fig. 3 presents the BER performance of an OOK underwater VLC system under different turbulence strengths (weak, moderate, and strong) for multiple and single LED arrangements. As observed, increased turbulence (lower values of k) leads to larger BER due to more intense signal fading. Multiple LEDs significantly improve BER performance compared to a single LED as spatial diversity can combat the impacts of turbulence. At high SNR values, the BER of multi-LED under weak turbulence (K=10) falls below 10^{-4}, indicating near error-free transmission. On the contrary, strong turbulence (k=0.8) with single LED offers the worst performance with relatively high BER even at high SNR. This analysis brings to light that the deployment of multi-LED in underwater VLC systems enhances reliability, especially in turbulent channels.

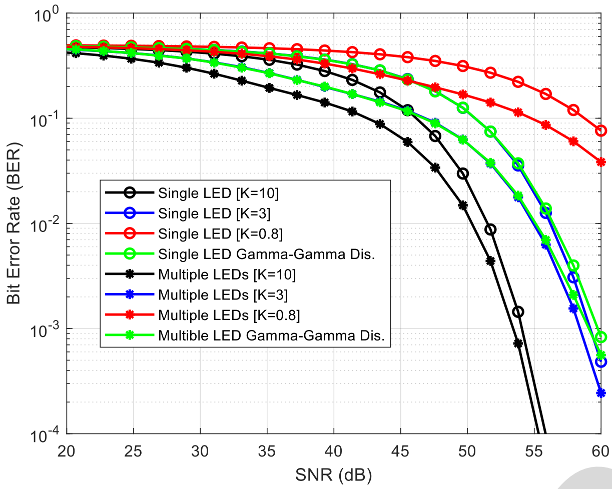

Fig. 2: BER for BPSK versus SNR at different cases of turbulence.

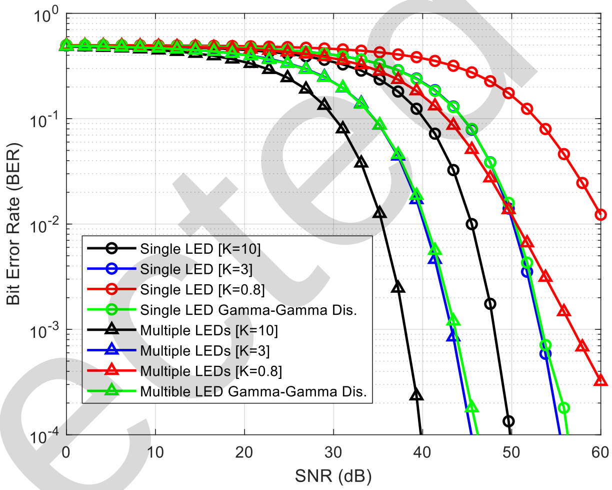

Fig. 3: BER for OOK versus SNR at different cases of Turbulence.

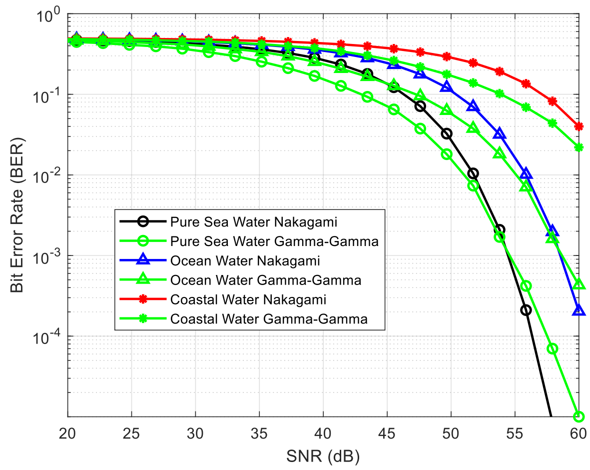

(a)

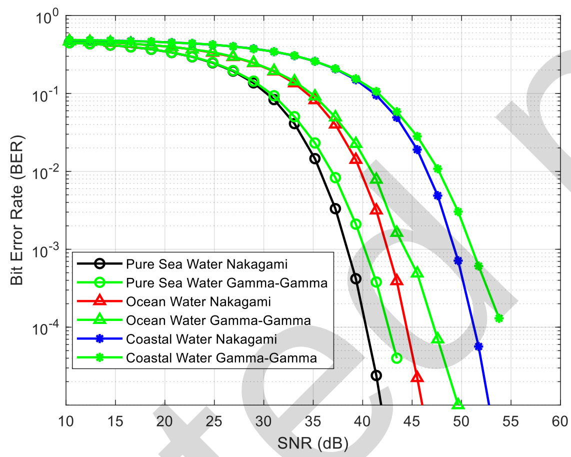

(b)

Fig. 4: BER for BPSK versus SNR at different water types (a- single LED, b- multiple LEDs).

Fig. 4 explores the BER performance of the BPSK considering different water types such as pure sea water, ocean water and costal water and keeping the turbulent intensity parameter to moderate level [k = 3]. Results for a single LED configuration are shown in subfigure (a). The one with the worst BER performance is the coastal water and then the ocean water and pure sea water. Subfigure (b) compares the performance with additional LEDs, which significantly improves the overall detection result for all water types. In pure and ocean water, BER decreases to close to zero at high SNR. In the BER, even in the case of the coastal water, the ratio is much lower than when it is single LED. This demonstrates the joint advantage of BPSK modulation and space diversity in types of environments.

A similar water-type comparison for OOK modulated signals is shown in **Fig. 5**. Sub Figure a indicates that in the single-LED systems the BER is still kept high by all water types, with a higher value for the coastal water. The results are worse than BPSK, even though multiple LEDs are used (Subfig. (b)). This confirms that OOK is not useful in harsh environments containing scattering and turbulence and shows that BPSK is a better choice for robust UVLC system design. Our comparison has highlighted how, in addition to the turbulence model, the choice of modulation and the LED architecture have a direct impact on the practical reliability of a system.

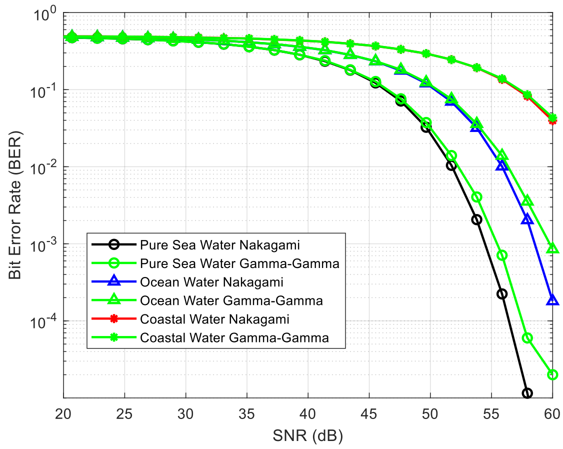

(a)

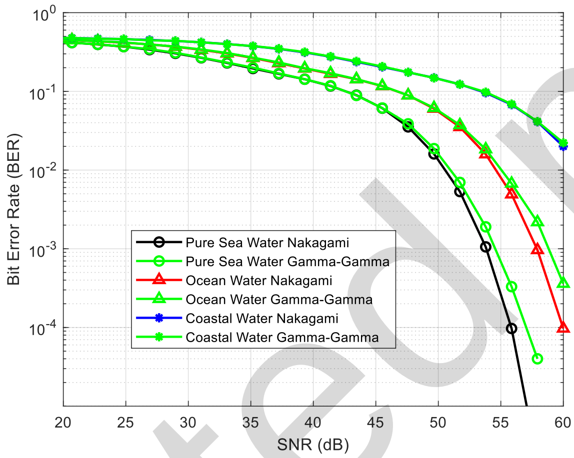

(b)

Fig. 5: BER for OOK versus SNR at different water types (a- single LED, b- multiple LEDs).

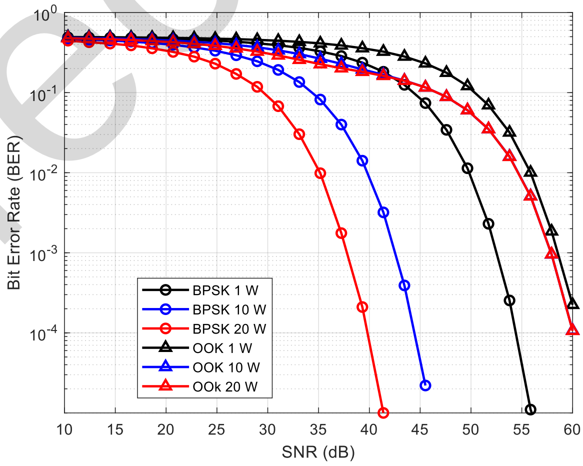

Fig. 6: The relation between power and BER for single LED.

When moderate turbulence phenomenon is modelled using the gamma-gamma distribution and results of [15] is compared, it is clearly seen from **Figs. 2 to 5** that our results can achieve a similar BER performance in both OOK, and BPSK modulation at k = 3. This alignment also verifies the applicability of the Nakagami model in moderate turbulence. Furthermore, figures also reveal that BPSK always outperforms OOK for same value of turbulence and exhibits lower BER for all values of SNR. This demonstrates the better reliability of BPSK in turbulent underwater channels.

Fig. 6 shows the BER performance of a single-LED UVLC system under varying transmitted power levels (1 W, 10 W and 20 W) using BPSK and OOK modulation formats. From the graph, It can be observed that there is an obvious tendency in BPSK: increasing the transmitted power remarkably decreases BER, notably at mid-high SNR values. For example, BPSK at 20 W at a BER of 10^{-4} is reached at about 40 dB SNR, whereas BPSK at 1 W would need some 55 dB SNR to reach a similar BER. In comparison, OOK modulation scheme has poor power scaling gain. Even at 20 W transmission, OOK still cannot get the same BER improvement as BPSK, which means OOK is more affected by the turbulence and cannot make good use of the power gain effectively. These results indicate the BPSK is more robust to power fluctuation and thus further confirm the BPSK is promising to the power-limited UVLC systems.

CONCLUSIONS

This research simulates and examines the impact of oceanic turbulence on UVLC systems using statistical modeling. Employing the Nakagami-k distribution to model the fading effect, we have calculated numerically the BER performance of OOK and BPSK modulation schemes for various regimes of turbulence (k = 0.8, 3, and 10) and for various types of water. Results indicate that turbulence severity has a reverse correlation with system reliability and that high turbulence (k = 0.8) causes BER degradation orders of magnitude in comparison to low turbulence (k = 10). Multi-LED systems, by spatial diversity, are far superior to single-LED systems and offer close-to-error-free transmission (BER $<10^{-4}$ at 40 dB SNR) in low turbulence and pure seawater. Oceanic water with higher scattering and absorption presented the greatest challenge and emphasized the need for adaptive turbid water designs. The results validate the need for turbulence-sensitive modeling and diversity techniques in the development of UVLC resilience for practical applications. More advanced modulation and error-correcting codes must be explored for higher spectral efficiency, and hybrid UVLC-acoustic/RF must be explored for a larger range, while machine learning-based adaptive algorithms must be created to predict turbulence. Experimental verification, power-efficient LED topologies, and integration with underwater sensor networks will ultimately drive UVLC to scalable and reliable underwater communications.

Water eddies, which are small swirling motions in water, can distort light paths and cause fluctuations in signal strength. These high-frequency variations differ from larger turbulence effects and can further degrade communication quality. Studying their impact will be part of future work.

REFERENCES

[1] K. Mittal, A. Gupta, N. Sharma, M. Jani, and P. Garg, "Performance Analysis of Hybrid RF/VLC Energy Harvested Terrestrial-Underwater System," IEEE Transactions on Sustainable Computing, vol. 9, no. 3, pp. 512–521, Nov. 2023, doi: 10.1109/tsusc.2023.3336374.

[2] R. Salam, A. Srivastava, V. A. Bohara, and A. Ashok, "An Optical Intelligent Reflecting Surface-Assisted Underwater Wireless Communication System," IEEE Open Journal of the Communications Society, vol. 4, pp. 1774–1786, Jan. 2023, doi: 10.1109/ojcoms.2023.3303190.

[3] R. Roshdy, A. Hussein, M. Mabrook, and M. Salem, "A complexity efficient PAPR reduction scheme for FBMC-based VLC systems," Opto-Electronics Review, Feb. 2023, doi: 10.24425/opelre.2023.144919.

[4] Y. Tang, X. Ding, Z. Li, C. Shao, Z. Huang, and S. Liang, "Crosstalk-Free MIMO VLC Using Two Orthogonal Polarizations Multiplexed Large FOV Fluorescent Antennas," IEEE Photonics Technology Letters, vol. 35, no. 23, pp. 1271–1274, Sep. 2023, doi: 10.1109/lpt.2023.3312327.

[5] A. Elfikky et al., "Underwater visible light communication: recent advancements and channel modeling," Optical and Quantum Electronics, vol. 56, no. 10, Sep. 2024, doi: 10.1007/s11082-024-07426-z.

[6] P. Zou, Y. Zhao, F. Hu, and N. Chi, "Underwater visible light communication at 3.24 Gb/s using novel two-dimensional bit allocation," Optics Express, vol. 28, no. 8, p. 11319, Mar. 2020, doi: 10.1364/oe.390718.

[7] E. E. Elsayed, "Performance enhancement of atmospheric turbulence channels in DWDM-FSO PON communication systems using M-ary hybrid DPPM-M-PAPM modulation schemes under pointing errors, ASE noise and interchannel crosstalk," Journal of Optics, 2024, doi:10.1007/s12596-024-01908-9

[8]] E. E. Elsayed, "Investigations on modified OOK and adaptive threshold for wavelength division multiplexing free-space optical systems impaired by interchannel crosstalk, atmospheric turbulence, and ASE noise," Journal of Optics, 2024, doi:10.1007/s12596-024-01929-4

[9] M. Elamassie, S. M. Sait, and M. Uysal, "Effect of Sea Waves on Vertical Underwater Visible Light Communication Links," IEEE Journal of Oceanic Engineering, vol. 48, no. 2, pp. 515–525, Nov. 2022, doi: 10.1109/joe.2022.3211286.

[10] R. Hamagami, T. Ebihara, N. Wakatsuki, and K. Mizutani, "Underwater Visible Light Communication Using Phase-Shift Keying and Rolling-shutter Effect," 2022 IEEE 11th Global Conference on Consumer Electronics (GCCE), pp. 842–843, Oct. 2020, doi: 10.1109/gcce50665.2020.9291709.

[11] L. Almonacid et al., On the Path Loss Performance of Underwater Visible Light Communication Schemes Evaluated in Several Water Environments. 2023, pp. 12–16. doi: 10.1109/sacvlc59022.2023.10347786.

[12] M. Uysal, S. Ghasvarianjahromi, M. Karbalayghareh, P. D. Diamantoulakis, G. K. Karagiannidis, and S. M. Sait, "SLIPT for Underwater Visible Light Communications: Performance Analysis and Optimization," IEEE Transactions on Wireless Communications, vol. 20, no. 10, pp. 6715–6728, May 2021, doi: 10.1109/twc.2021.3076159.

[13] J. Liu, L. Ma, and Z. He, "Underwater Visible Light Mobile Communication Using a Gain Feedback Control Method With Dynamic Threshold," IEEE Photonics Journal, vol. 15, no. 6, pp. 1–6, Nov. 2023, doi: 10.1109/jphot.2023.3333227.

[14] G. K. Varotsos, H. E. Nistazakis, E. Kapotis, E. V. Chatzikontis, K. Aidinis, and C. K. Volos, ABER Estimation of NLOS UV Links with Time Diversity over K-Turbulent Channels and Path Loss. 2023, pp. 1–4. doi: 10.1109/mocast57943.2023.10176401.

[15] P. Pandey and M. Agrawal, Performance Evaluation of Underwater Visible Light Communication System for Strong Oceanic Turbulence Channel. 2023, pp. 1–5. doi: 10.1109/oceanslimerick52467.2023.10244701.

[16] F. Zhang, J. Luo, J. Li, T. Lin, C. Gong, and Z. Xu, "Effects of underwater swing nodes on water-to-air visible light communication," Applied Optics, vol. 62, no. 16, p. 4245, May 2023, doi: 10.1364/ao.488754.

[17] X. Li, L. Sun, J. Huang, and F. Zeng, "Channel Polarization Scheme for Ocean turbulence channels in underwater visible light communication," Journal of Marine Science and Engineering, vol. 11, no. 2, p. 341, Feb. 2023, doi: 10.3390/jmse11020341.

[18] F. Miramirkhani and M. Uysal, "Visible Light Communication channel modeling for underwater environments with blocking and shadowing," IEEE Access, vol. 6, pp. 1082–1090, Nov. 2017, doi: 10.1109/access.2017.2777883.

[19] N. Monzon, D. Gutierrez, D. Akkaynak, and A. Muñoz, "Real-Time Underwater Spectral Rendering," Computer Graphics Forum, vol. 43, no. 2, Apr. 2024, doi: 10.1111/cgf.15009.

[20] Jiang Hongyan, Qiu Hongbing, He Ning, Wu Yue, Z. A. Z. Ahmad, and S. R. S. Rajbhandari, "Optical OFDM spatial diversity system in lognormal fading UVLC channels," Infrared and Laser Engineering, vol. 49, no. 2, p. 203008, Jan. 2020, doi: 10.3788/irla202049.0203008.

[21] M. De Oliveira, F. C. B. Tosta, D. E. F. Guillen, P. P. Monteiro, and A. De Almeida Prado Pohl, "Theoretical and experimental analysis of LED lamp for visible light communications," Wireless Personal Communications, vol. 125, no. 4, pp. 3461–3477, May 2022, doi: 10.1007/s11277-022-09720-z.

[22] C. Wang, H.-Y. Yu, and Y.-J. Zhu, "A long distance underwater visible light communication system with single photon avalanche diode," IEEE Photonics Journal, vol. 8, no. 5, pp. 1–11, Aug. 2016, doi: 10.1109/jphot.2016.2602330.

[23] Z. Ghassemlooy, W. Popoola, and S. Rajbhandari, Optical Wireless Communications: System and Channel Modelling with MATLAB®, Second Edition. 2019. [Online]. Available: http://cds.cern.ch/record/2293266

[24] M. F. Ali, D. N. K. Jayakody, and Y. Li, "Recent trends in underwater Visible Light Communication (UVLC) systems," IEEE Access, vol. 10, pp. 22169–22225, Jan. 2022, doi: 10.1109/access.2022.3150093.

[25] Spagnolo, G.S.; Cozzella, L.; Leccese, F. A Brief Survey on Underwater Optical Wireless Communications. In Proceedings of the MetroSea 2020-TC19 International Workshop on Metrology for the Sea, Naples, Italy, 5–7 October 2020; pp. 79–84. Available online: **https://www.imeko.org/publications/tc19-Metrosea-2020/**

[26] M. Furqan Ali and D. N. K. Jayakody, "SIMO-Underwater Visible Light Communication (UVLC) system," Computer Networks, vol. 232, p. 109750, Aug. 2023, doi: 10.1016/j.comnet.2023.109750.